Pairwise atomic states: Two-atom system in a three-dimensional squeezed vacuum field

Z. Ficek*
Department of Physics, The University of Queensland, Queensland 4072, Australia
(Received 16 May 1991)

We analyze the pairwise atomic states that are produced when a system of two atoms is irradiated by a squeezed vacuum field. Included in the analysis is the three-dimensional squeezed vacuum field propagated over a solid angle Ω, the interatomic separation r_{12}, the microscopic Fabry-Pérot cavity, and the role played by an imperfect coupling between the cavity modes and squeezed input modes. It is shown that the steady state of the system in free space is the pairwise atomic state when the atoms interact with a perfect squeezed dipole wave and the interatomic separations are much smaller than the resonant wavelength (Dicke model). With the interatomic separations comparable to the resonant wavelength or with an imperfect squeezed dipole wave, the system decays to a state that is not the pairwise atomic state. The effect of squeezed vacuum field on the system is now manifested by the selective population of the collective atomic states. For atoms inside a microscopic Fabry-Pérot cavity the pairwise atomic states are produced with an imperfect squeezed dipole wave. This can occur even for small solid angles Ω. However, this effect is sensitive to mode matching between internal and external fields. It is shown that with a Gaussian profile for the input squeezed modes the steady state is not the pairwise atomic states, but a significant reduction of the population in the symmetric state still can be observed.

PACS number(s): 42.50.Dv, 42.50.Fx

I. INTRODUCTION

The interaction of squeezed radiation with atomic systems has been attracting considerable attention during the past few years [1–6]. In the field of atomic spectroscopy, the introduction of a squeezed vacuum field to a number of classic problems has led to predictions of novel and unusual effects. New phenomena predicted in the interaction of a squeezed vacuum field with atomic systems have included the inhibition of atomic phase decays [1,2], a well-defined phase in a squeezed pump laser [3], subnatural linewidth spectroscopy [4], two-photon absorption [5], and squeezing-induced population inversion [6]. The results show that there exist some essential distinctions between a squeezed field and the ordinary vacuum field. The distinctions originate from the fact that the squeezed field contains strong internal two-photon correlations, which can be produced by a parametric amplifier [7]. In a parametric amplifier an intense laser beam at frequency 2ω—the pump beam—illuminates a suitable nonlinear medium. The nonlinearity couples the pump beam to other modes of the electromagnetic field in such a way that a pump photon at frequency 2ω can be annihilated to create strongly correlated pairs of photons at frequencies $\omega\pm\epsilon$. These correlations lead to the unequal partition of the quantum noise between two quadrature components $E_1(t)$ and $E_2(t)$ of the electromagnetic field $E(t)$ emitted by the parametric amplifier. In the above works [1–6] an effective two- or three-level atom interacted with such a squeezed vacuum field.

The interaction of a collection of atoms with the squeezed vacuum field also leads to a number of novel and interesting phenomena. These show some very interesting deviations from the ordinary decay and ordinary emission spectra. In particular, the multiatom resonance fluorescence spectrum, apart from a subnatural or supernatural linewidth of the components [8] observed in a single atom spectrum, demonstrates an asymmetry under off-resonance excitation by an external coherent laser field [9]. The two-atom Dicke model interacting with a squeezed vacuum field may generate a new class of states, which satisfy the equality sign in the Heisenberg uncertainty relation for angular-momentum operators [10,11]. Moreover, in the squeezed vacuum field the total atomic population can decay to a pure state in which the atoms are populated in pairs. This pure state named as a pairwise atomic state [12] is also known as two-atom squeezed state [13]. In this state the collective atomic states are not all excited [12]. A pair of two-level atoms separated by a distance r_{12} that is much smaller than their resonant wavelength (Dicke model) can be represented by a single three-level system [14], with the ground state $|1\rangle$, the intermediate superradiant state $|+\rangle$, and the upper state $|2\rangle$. When this system is in the pairwise atomic state, the superradiant state $|+\rangle$ is not populated [12]. The system is then in the state which is a coherent superposition of the ground state $|1\rangle$ and the upper state $|2\rangle$.

To obtain the pairwise atomic states an ideal coupling between the atoms and the squeezed vacuum field has been assumed. In this case the atoms interact only with a one-dimensional multimode squeezed radiation field, with no interactions or spontaneous emission into ordinary (unsqueezed) vacuum modes. This assumption, however, may prove difficult in experimental realization. It would be realized in practice using some type of waveguide or generating of a squeezed perfect electric dipole wave. In atomic spectroscopy, however, the experiments usually

 ©1991 The American Physical Society

use atomic-beam methods [15,16], where the atoms interact with an incoming wave that is not a perfect electric dipole. In this case the atoms interact not only with the incoming field, which can be in the squeezed state, but also with the ordinary vacuum modes. The presence of the unsqueezed modes can completely mask the effects induced by the squeezed vacuum field [1,6]. Recently, Parkins and Gardiner [2] have discussed the inhibition of atomic phase decays by squeezed light, and have shown that this difficulty can be eliminated by use of a microscopic Fabry-Pérot cavity. In the microscopic Fabry-Pérot cavity a strong selection of radiation modes coupling to atoms within the cavity is possible [17], and by squeezing of these selected modes we can achieve an effective squeezed vacuum-atom coupling despite the presence of unsqueezed modes.

In this paper we consider the interaction between two two-level atoms and the three-dimensional vacuum field in which some modes can be squeezed. We discuss in detail the possibility of obtaining an experimental realization of the pairwise atomic states. As it has been mentioned earlier the pairwise atomic states are manifested by zero steady-state population of the superradiant state $|+\rangle$. Because fluorescence from the state $|+\rangle$ is proportional to the population of this state, one can observe this effect by monitoring the intensity of the fluorescence from the state $|+\rangle$. In Sec. II we derive the master equation for the reduced intensity operator ρ of the two-atom system interacting with the incident squeezed vacuum field. We assume that the atoms are coupled to the three-dimensional field and the incident squeezed vacuum field is propagated over a solid angle Ω. We also allow spontaneous emission into the unsqueezed modes. In Sec. III we obtain solutions for the steady-state population of the superradiant state $|+\rangle$ when the two-atom Dicke model in free space interacts with the squeezed vacuum field. In Sec. IV we discuss the effect of the interatomic separation r_{12} on the population of the state $|+\rangle$, and on the pairwise atomic state. In Sec. V we obtain solutions for the population in the state $|+\rangle$ when the atoms interact inside the microscopic Fabry-Pérot cavity with the squeezed vacuum field. We assume a perfect matching between the incident squeezed modes and the cavity modes. In Sec. VI we examine the effect of an imperfect matching on the pairwise atomic states. We assume that the incident squeezed field has a Gaussian profile. In Sec. VII we summarize our results.

II. MASTER EQUATION

We consider a system of two identical atoms, separated by a distance r_{12} and interacting with the quantized multimode three-dimensional field. Each atom is modeled as a two-level system with the ground state $|1\rangle_i$ and the excited state $|2\rangle_i$ $(i=1,2)$. The Hamiltonian of the system in the electric dipole approximation has the following form:

$$H=H_0+H_{\rm int} , \tag{1}$$

with

$$H_0=\tfrac{1}{2}\hbar\omega_0\sum_{i=1}^{2}[S_{22}^{(i)}-S_{11}^{(i)}]+\hbar c\sum_s\int|\mathbf{k}|a^\dagger(\mathbf{k},s)a(\mathbf{k},s)d^3\mathbf{k} \tag{1a}$$

and

$$H_{\rm int}=i\hbar\sum_s\sum_{i=1}^{2}\sum_{\substack{m,n=1\\ m\neq n}}^{2}\int[\boldsymbol{\mu}_{mn}\cdot\mathbf{g}_{\mathbf{k}s}(\mathbf{r}_i)a(\mathbf{k},s)S_{mn}^{(i)} +\text{H.c.}]d^3\mathbf{k} , \tag{1b}$$

where ω_0 is the atomic resonance frequency, and $S_{mn}^{(i)}=|m\rangle_{ii}\langle n|$ are pseudospin operators for the ith atom satisfying the well-known commutation relations

$$[S_{mn}^{(i)},S_{pq}^{(j)}]=[S_{mq}^{(i)}\delta_{np}-S_{pn}^{(i)}\delta_{qm}]\delta_{ij} . \tag{2}$$

In Eq. (1), $\boldsymbol{\mu}_{mn}=\langle m|\boldsymbol{\mu}|n\rangle$ is the electric dipole moment transition matrix element between the atomic states $|m\rangle$ and $|n\rangle$, s is the polarization index $(s=1,2)$, and $\mathbf{g}_{\mathbf{k}s}(\mathbf{r}_i)$ is the appropriate mode function, evaluated at the position of the ith atom. This mode function describes coupling between the atoms and the quantized three-dimensional electromagnetic field, and can have a different structure depending on the configuration of interaction between atoms and the field.

The operators $a(\mathbf{k},s)$ and $a^\dagger(\mathbf{k},s)$, which appear in Eq. (1), describe a three-dimensional electromagnetic field, which can be in a squeezed state. In the general case such a three-dimensional field can be defined by the commutation and correlations relations [6,18]

$$\begin{aligned}&[a(\mathbf{k},s),a^\dagger(\mathbf{k}',s')]=\delta^3(\mathbf{k}-\mathbf{k}')\delta_{ss'} ,\\ &\langle a^\dagger(\mathbf{k},s)a(\mathbf{k}',s')\rangle=n(\mathbf{k},s;\mathbf{k}',s') ,\\ &\langle a(\mathbf{k},s)a(\mathbf{k}',s')\rangle=m(\mathbf{k},s;\mathbf{k}',s') .\end{aligned} \tag{3}$$

In the above equation $n(\mathbf{k},s;\mathbf{k}',s')$ and $m(\mathbf{k},s;\mathbf{k}',s')$ are photon number and squeezing densities, respectively, in momentum space, whose explicit form depends on the preparation and propagation of the squeezed vacuum field. Let us assume that the squeezed field propagates along the z axis and only those modes whose propagation vectors $\mathbf{k}$ have an angle θ_k with the z axis less than a maximum value θ are squeezed. All other modes are not squeezed. This can be achieved by defining the squeezing parameters $n(\mathbf{k},s;\mathbf{k}'s')$ and $m(\mathbf{k},s;\mathbf{k}',s')$ as [2,6]

$$\begin{aligned}&n(\mathbf{k},s;\mathbf{k}',s')=N(k)U_s^*(\mathbf{k})U_{s'}(\mathbf{k}')\delta(k-k')/k^2 ,\\ &m(\mathbf{k},s;\mathbf{k}',s')=M(k)U_s(\mathbf{k})U_{s'}(\mathbf{k}')\delta(2k_0-k-k')/kk' ,\end{aligned} \tag{4}$$

where $k_0=\omega/c$, where ω is the carrier frequency of the squeezing; $N(k)$ and $M(k)=M(2k_0-k)=|M(k)|\exp(i\varphi_v)$ are parameters characterizing the squeezing such that $|M(k)|^2\leq N(k)[N(k)+1]$, where the equality holds for a minimum-uncertainty squeezed states, and φ_v is the phase of the squeezed vacuum field. In Eq. (4), $U_s(\mathbf{k})$ is defined as a square normalized mode function of the input squeezed field that includes only directions $\mathbf{k}$ confined to a solid angle $\Omega_k=(\theta_k,\varphi_k)$ with equal amplitude. This mode function depends on the angle of propagation, and can have a different structure de-

pending on the method of propagation and focusing of the squeezed field. In particular, it may be chosen to optimize the coupling between the atoms and the input field. In this case, the mode structure of the squeezed field incident on the atoms is perfectly matched to the mode structure $\mathbf{g}_{ks}(\mathbf{r})$, which describes coupling of the three-dimensional field with the atoms. With the optimal matching the mode function $U_s(\mathbf{k})$ can be chosen as

$$U_s(k)=\begin{cases}[\mathcal{N}(k)]^{-1/2}\boldsymbol{\mu}^*\cdot\mathbf{g}^*_{ks}(\mathbf{r}_0) & \text{for } \theta_k\le\theta \\ 0 & \text{for } \theta_k>\theta\ ,\end{cases} \tag{5}$$

where $\mathbf{r}_0=(r_x^{(s)},r_y^{(s)},r_z^{(s)})$ is a coordinate of a point at which the squeezed field is focused. In general, $\mathbf{r}_0$ can be different from a point $\mathbf{r}_i$ at which ith atom is located. In Eq. (5), $\mathcal{N}(k)$ is the normalization constant defined so that $U_s(\mathbf{k})$ is dimensionless, with

$$\mathcal{N}(k)=\int_\Omega d\Omega_k\sum_s|\boldsymbol{\mu}\cdot\mathbf{g}_{ks}(\mathbf{r}_0)|^2\ , \tag{6}$$

where Ω is the total solid angle over which the squeezing is incident.

A master equation for the reduced density operator ρ of the two-atom system interacting with the quantized three-dimensional electromagnetic field is derived from the Hamiltonian (1). It can be derived using any of a number of traditional techniques [19,20].

We apply a Born-Markov method [21–23] adapted to the situation of a nonstationary reservoir. The time evolution of the density operator $W(t)$ of the atom-field system in the interaction picture obeys the equation

$$i\hbar\frac{\partial}{\partial t}W^I(t)=[H^I_{\rm int}(t),W^I(t)]\ , \tag{7}$$

where $H_{\rm int}$ is given by Eq. (1b), and the superscript I stands for operators in the interaction picture.

Formally integrating Eq. (7) gives

$$W^I(t)=W^I(0)+\frac{1}{i\hbar}\int_0^t dt'[H^I_{\rm int}(t'),W^I(t')]\ . \tag{8}$$

Substituting this solution into the right-hand side of Eq. (7), and taking the trace over the reservoir states of each side of Eq. (7), we get

$$\begin{aligned}i\hbar\frac{\partial}{\partial t}\rho^I(t)&=\mathrm{Tr}_R[H^I_{\rm int}(t),W(0)]\\&\quad+\frac{1}{i\hbar}\int_0^t dt'\mathrm{Tr}_R[H^I_{\rm int}(t),[H^I_{\rm int}(t'),W^I(t')]]\ ,\end{aligned} \tag{9}$$

where $\rho^I(t)=\mathrm{Tr}_R\,W^I(t)$ is the reduced density operator of the atomic system.

We choose an initial state with no correlations between the atomic system and the squeezed field, i.e., $W^I(0)=\rho^I(0)\rho_R(0)$, where $\rho_R(0)$ is the density operator for the field reservoir. We also assume that the interaction Hamiltonian satisfies the condition [22,23]

$$\mathrm{Tr}_R[H^I_{\rm int}(t)\rho_R(0)]=0\ . \tag{10}$$

This can easily be arranged. The left-hand side of Eq. (10) is a system operator. If the left-hand side of Eq. (10) were nonzero, the system Hamiltonian could be altered to include part in $H_{\rm int}$ so that when added to the left-hand side of Eq. (10) zero occurs. The condition (10) can apply even in the case where the freely evolving reservoir density operator $\rho_R(t)$ changes with time, as occurs for the squeezed reservoir [1–4,19]. On the basis of these assumptions Eq. (9) reduces to

$$\frac{\partial}{\partial t}\rho^I(t)+\frac{1}{\hbar^2}\int_0^t dt'\mathrm{Tr}_R[H^I_{\rm int}(t),[H^I_{\rm int}(t'),W^I(t')]]=0\ . \tag{11}$$

We now employ the Born approximation in which the atom-field interaction is supposed to be weak [24,25]. With this approximation we can write

$$W^I(t')=\rho^I(t')\rho_R(0)\ , \tag{12}$$

and after changing time variable to $t'=t-\tau$, Eq. (11) simplifies to

$$\frac{\partial}{\partial t}\rho^I(t)+\frac{1}{\hbar^2}\int_0^t d\tau\,\mathrm{Tr}_R[H^I_{\rm int}(t),[H^I_{\rm int}(t-\tau),\rho_R(0)\rho^I(t-\tau)]]=0\ . \tag{13}$$

After a Laplace transform over time t, with (1b) and (3), Eq. (13) leads to (ignoring the superscript I)

$$\begin{aligned}\rho(0)-z\rho(z)&=\sum_{i,j}[\eta_{ij}(z)-i\Omega^{(M)}_{ij}(z)]\{[S_j^+,\rho(z)S_i^+]+[S_i^+\rho(z),S_j^+]\}\\&\quad+\sum_{i,j}[\eta^*_{ij}(z)+i\Omega^{(M)*}_{ij}(z)]\{[S_j^-,\rho(z)S_i^-]+[S_i^-\rho(z),S_j^-]\}\\&\quad+\sum_{i,j}\beta_{ij}(z)[\rho(z)S_j^-S_i^++S_j^-S_i^+\rho(z)-2S_i^+\rho(z)S_j^-]\\&\quad+\sum_{i,j}[\beta_{ij}(z)+\gamma_{ij}(z)][\rho(z)S_i^+S_j^-+S_i^+S_j^-\rho(z)-2S_j^-\rho(z)S_i^+]\\&\quad+i\sum_i[\Omega_{ii}(z)+2\Omega^{(N)}_{ii}(z)][S_i^+S_i^-,\rho(z)]+i\sum_{\substack{i,j\\i\neq j}}\Omega_{ij}(z)[S_i^+S_j^-,\rho(z)]\ .\end{aligned} \tag{14}$$

Here $\rho(z)$ is the Laplace transform of $\rho(t)$, and the parameters are given by

$$\eta_{ij}(z)=\frac{1}{c}\sum_{s,s'}\int\int[\boldsymbol{\mu}\cdot\mathbf{g}_{\mathbf{k}s}(\mathbf{r}_i)][\boldsymbol{\mu}\cdot\mathbf{g}_{\mathbf{k}'s'}(\mathbf{r}_j)]\frac{m(\mathbf{k},s;\mathbf{k}',s')(z/c)}{(z/c)^2+(k_0-k)^2}d^3\mathbf{k}\,d^3\mathbf{k}',$$

$$\beta_{ij}(z)=\frac{1}{c}\sum_{s,s'}\int\int[\boldsymbol{\mu}^*\cdot\mathbf{g}^*_{\mathbf{k}s}(\mathbf{r}_i)][\boldsymbol{\mu}\cdot\mathbf{g}_{\mathbf{k}'s'}(\mathbf{r}_j)]\frac{n(\mathbf{k},s;\mathbf{k}',s')(z/c)}{(z/c)^2+(k_0-k)^2}d^3\mathbf{k}\,d^3\mathbf{k}',$$

$$\gamma_{ij}(z)=\frac{1}{c}\sum_{s}\int[\boldsymbol{\mu}^*\cdot\mathbf{g}^*_{\mathbf{k}s}(\mathbf{r}_i)][\boldsymbol{\mu}\cdot\mathbf{g}_{\mathbf{k}s}(\mathbf{r}_j)]\frac{(z/c)}{(z/c)^2+(k_0-k)^2}d^3\mathbf{k},$$

$$\Omega^{(M)}_{ij}(z)=\frac{1}{c}\sum_{s,s'}\int\int[\boldsymbol{\mu}\cdot\mathbf{g}_{\mathbf{k}s}(\mathbf{r}_i)][\boldsymbol{\mu}\cdot\mathbf{g}_{\mathbf{k}'s'}(\mathbf{r}_j)]\frac{m(\mathbf{k},s;\mathbf{k}',s')(k-k_0)}{(z/c)^2+(k-k_0)^2}d^3\mathbf{k}\,d^3\mathbf{k}', \tag{15}$$

$$\Omega^{(N)}_{ii}(z)=\frac{1}{c}\sum_{s,s'}\int\int n(\mathbf{k},s;\mathbf{k}'s')[\boldsymbol{\mu}\cdot\mathbf{g}_{\mathbf{k}s}(\mathbf{r}_i)][\boldsymbol{\mu}\cdot\mathbf{g}_{\mathbf{k}'s'}(\mathbf{r}_i)]\left[\frac{(k-k_0)}{(z/c)^2+(k-k_0)^2}-\frac{(k_0+k)}{(z/c)^2+(k_0+k)^2}\right]d^3\mathbf{k}\,d^3\mathbf{k}',$$

$$\Omega_{ii}(z)=\frac{1}{c}\sum_{s}\int|\boldsymbol{\mu}\cdot\mathbf{g}_{\mathbf{k}s}(\mathbf{r}_i)|^2\left[\frac{(k-k_0)}{(z/c)^2+(k-k_0)^2}-\frac{(k_0+k)}{(z/c)^2+(k_0+k)^2}\right]d^3\mathbf{k},$$

$$\Omega_{ij}(z)=\frac{1}{c}\sum_{s}\int[\boldsymbol{\mu}^*\cdot\mathbf{g}^*_{\mathbf{k}s}(\mathbf{r}_i)][\boldsymbol{\mu}\cdot\mathbf{g}_{\mathbf{k}s}(\mathbf{r}_j)]\left[\frac{(k-k_0)}{(z/c)^2+(k-k_0)^2}+\frac{(k_0+k)}{(z/c)^2+(k_0+k)^2}\right]d^3\mathbf{k},$$

where z is the complex Laplace transform parameter, and $\boldsymbol{\mu}=\boldsymbol{\mu}_{21}$. To obtain Eq. (14) we have used the commutation relations (2) and made the rotating-wave approximation [26], i.e., we neglected rapidly oscillating terms with frequency $2\omega_0$ (the so-called counterrotating terms). In Eq. (14) we have also introduced a shorter notation for the atomic operators, i.e.,

$$S_i^+=S_{21}^{(i)}=|2\rangle_{ii}\langle 1|,\quad S_i^-=(S_i^+)^\dagger. \tag{16}$$

Now we employ the Markov approximation. This neglects retardation effects [27] and is valid in the long-time limit $t\gg\omega_0^{-1}$, providing this is short compared with the typical relaxation times of the system. Moreover, we assume that the bandwidth of squeezing is to be sufficiently broad that the squeezed field appears as δ-correlated squeezed white noise to the atoms. With these approximations we can replace the $\eta(z)$, $\beta(z)$, $\gamma(z)$, and $\Omega(z)$ parameters by their limiting values as $z\rightarrow 0+$. After this, and using Eq. (4), the inverse Laplace transform of Eq. (14) leads to the master equation

$$\frac{\partial\rho}{\partial t}=-M\sum_{i,j}\eta_{ij}([S_i^+,\rho S_j^+]+[S_j^+\rho,S_i^+])-M^*\sum_{i,j}\eta^*_{ij}([S_i^-\rho,S_j^-]+[S_j^-,\rho S_i^-])$$

$$-N\sum_{i,j}\beta_{ij}(\rho S_i^-S_j^++S_i^-S_j^+\rho-2S_j^+\rho S_i^-)-\sum_{i,j}(\gamma_{ij}+N\beta_{ij})(\rho S_i^+S_j^-+S_i^+S_j^-\rho-2S_j^-\rho S_i^+)-i\sum_{\substack{i,j\\ i\neq j}}\Omega_{ij}[S_i^+S_j^-,\rho], \tag{17}$$

where $M=M(k_0)$, $N=N(k_0)$, and the coefficients in the equation are

$$\eta_{ij}=\frac{\pi k_0^2}{c}\left[\int_\Omega d\Omega_k \sum_s U_s(\mathbf{k})[\boldsymbol{\mu}\cdot\mathbf{g}_{\mathbf{k}s}(\mathbf{r}_i)]\right]\times\left[\int_\Omega d\Omega_{k'}\sum_{s'} U_{s'}(\mathbf{k}')[\boldsymbol{\mu}\cdot\mathbf{g}_{\mathbf{k}',s'}(\mathbf{r}_j)]\right],$$

$$\beta_{ij}=\frac{\pi k_0^2}{c}\left[\int_\Omega d\Omega_k \sum_s U_s^*(\mathbf{k})[\boldsymbol{\mu}^*\cdot\mathbf{g}_{\mathbf{k}s}^*(\mathbf{r}_i)]\right]\times\left[\int_\Omega d\Omega_{k'}\sum_{s'} U_{s'}(\mathbf{k}')[\boldsymbol{\mu}\cdot\mathbf{g}_{\mathbf{k}',s'}(\mathbf{r}_j)]\right], \tag{18}$$

$$\gamma_{ij}=\frac{\pi k_0^2}{c}\int d\Omega_k \sum_s [\boldsymbol{\mu}^*\cdot\mathbf{g}_{\mathbf{k}s}^*(\mathbf{r}_i)][\boldsymbol{\mu}\cdot\mathbf{g}_{\mathbf{k}s}(\mathbf{r}_j)],$$

$$\Omega_{ij}=-\frac{1}{c}\int dk\, k^2\left[\frac{1}{k-k_0}+\frac{1}{k+k_0}\right]\times\int d\Omega_k\sum_s [\boldsymbol{\mu}^*\cdot\mathbf{g}_{\mathbf{k}s}^*(\mathbf{r}_i)][\boldsymbol{\mu}\cdot\mathbf{g}_{\mathbf{k}s}(\mathbf{r}_j)].$$

In the derivation of Eq. (17) we have assumed that the carrier frequency of the squeezed vacuum field is in resonance with the frequency ω_0 of the atomic transition, i.e., $\omega_0=\omega$. Moreover, we have ignored the parameters $\Omega_{ij}^{(M)}$, $\Omega_{ii}^{(N)}$, and Ω_{ii}, as they are negligibly small [28] compared to the Ω_{ij} term, which represents the dipole-dipole interaction between the atoms.

Our master equation (17) is fundamental for the theory of radiation of two atoms interacting with a three-dimensional field in which part of the modes can be squeezed. This is quite general, in terms of mode functions $\mathbf{g}_{\mathbf{k}s}(\mathbf{r})$ and $U_s(\mathbf{k})$, although it requires that the correlation functions of squeezed modes be much broadband than the decay constants of the system. For the normal vacuum ($N=|M|=0$) it is the same as those derived by Agarwal [20]. For isotropic systems, in which all modes coupled to the atoms are squeezed, and for the interatomic separations much smaller than the resonant wavelength ($\eta_{ij}=\beta_{ij}=\gamma_{ij}=\gamma$), the master equation (17) reduces to those obtained by Agarwal and Puri [12]. In the following sections we apply the master equation (17) to different theoretical and experimental schemes which can be used to produce the pairwise atomic states.

III. TWO-ATOM DICKE MODEL IN FREE SPACE

When two identical two-level atoms are separated by a distance r_{12} that is smaller than their resonant wavelength λ, cooperative decay phenomena can occur. Dicke [14] has found that the exchange of photons between the two atoms produces new eigenstates with new decay rates. In the framework of these states, called as a collective atomic states, the two-atom system is equivalent to a single four-level system (Fig. 1) with one upper state $|2\rangle=|2\rangle_1|2\rangle_2$, one ground state $|1\rangle=|1\rangle_1|1\rangle_2$, and two intermediate states: a superradiant state $|+\rangle=(1/\sqrt{2})(|2\rangle_1|1\rangle_2+|1\rangle_1|2\rangle_2)$, and a subradiant state $|-\rangle=(1/\sqrt{2})(|2\rangle_1|1\rangle_2-|1\rangle_1|2\rangle_2)$, where $|2\rangle_i$ and $|1\rangle_i$ denote, respectively, the excited and ground states of the ith atom. The triplet states $|1\rangle$, $|+\rangle$, and $|2\rangle$ are symmetrical, while the single state $|-\rangle$ is antisymmetric under the exchange $1\leftrightarrow 2$. When the interatomic separation r_{12} is much smaller than the resonant wavelength ($k_0 r_{12}\ll 1$), the antisymmetric state $|-\rangle$ is completely decoupled from the triplet states, and only symmetric states take part in the interaction with the electromagnetic field. In this case, the two-atom system is equivalent to the three-level cascade system, and is referred to as the small-sample model or two-atom Dicke model. In our model such a two-atom system interacts with the squeezed vacuum field. The one-dimensional calculation shows [12] that in the steady state and for a minimum-uncertainty squeezed states the superradiant state $|+\rangle$ is completely unpopulated. The two-atom system is then in the pairwise atomic state which is a coherent superposition of the states $|1\rangle$ and $|2\rangle$. Here we consider the steady-state population of the superradiant state $|+\rangle$ when the two-atom Dicke model interacts in free space with a three-dimensional field, in which part of the modes is squeezed. First, we derive general formulas for the coefficients of the master equation (17), when the two-atom system interacts in free space with the electromagnetic field in which part of the modes is squeezed. Next, we shall approximate these formulas to the two-atom Dicke model.

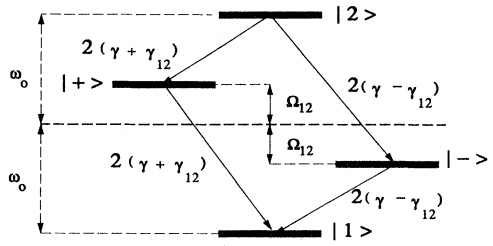

FIG. 1. Energy diagram for the collective atomic states, showing the frequency shift Ω_{12} and decay constants $2(\gamma\pm\gamma_{12})$.

For a three-dimensional multimode field in free space, the mode function $\mathbf{g}_{\mathbf{k}s}(\mathbf{r}_i)$ is defined as (in SI units)

$$\mathbf{g}_{\mathbf{k}s}(\mathbf{r}_i)=\left[\frac{ck}{2\epsilon_0\hbar(2\pi)^3}\right]^{1/2}\hat{\mathbf{e}}_{\mathbf{k}s}e^{i\mathbf{k}\cdot\mathbf{r}_i}, \tag{19}$$

where $\hat{\mathbf{e}}_{\mathbf{k}s}$ is the unit polarization vector, and $\mathbf{r}_i=(r_x^{(i)},r_y^{(i)},r_z^{(i)})$ is a coordinate of the ith atom. We assume that the mode function of the squeezed field is perfectly matched with the mode function (19). Moreover, for simplicity, we assume that the squeezed field is propagated along the z axis, and is focused at a point $\mathbf{r}_0=(0,0,r_z^{(s)})$. The atoms are at the positions $\mathbf{r}_1=(r_x^{(1)},0,r_z^{(1)})$ and $\mathbf{r}_2=(r_x^{(2)},0,r_z^{(2)})$. With these assumptions, and with Eqs. (5) and (19), the decay constants and the dipole-dipole interaction term in (18) are

$$\eta_{ij}=\frac{\mu^2k_0^3}{16\pi^2\epsilon_0\hbar}\frac{1}{\mathcal{N}'}\left[\int_\Omega d\Omega_k\sum_s|\hat{\boldsymbol{\mu}}\cdot\hat{\mathbf{e}}_{\mathbf{k}s}|^2e^{i\mathbf{k}\cdot(\mathbf{r}_i-\mathbf{r}_0)}\right]\times\left[\int_\Omega d\Omega_{k'}\sum_{s'}|\hat{\boldsymbol{\mu}}\cdot\hat{\mathbf{e}}_{\mathbf{k}'s'}|^2e^{i\mathbf{k}'\cdot(\mathbf{r}_j-\mathbf{r}_0)}\right],$$

$$\beta_{ij}=\frac{\mu^2k_0^3}{16\pi^2\epsilon_0\hbar}\frac{1}{\mathcal{N}'}\left[\int_\Omega d\Omega_k\sum_s|\hat{\boldsymbol{\mu}}\cdot\hat{\mathbf{e}}_{\mathbf{k}s}|^2e^{-i\mathbf{k}\cdot(\mathbf{r}_i-\mathbf{r}_0)}\right]\times\left[\int_\Omega d\Omega_{\mathbf{k}'}\sum_{s'}|\hat{\boldsymbol{\mu}}\cdot\hat{\mathbf{e}}_{\mathbf{k}'s'}|^2e^{i\mathbf{k}'\cdot(\mathbf{r}_j-\mathbf{r}_0)}\right], \tag{20}$$

$$\gamma_{ij}=\frac{\mu^2k_0^3}{16\pi^2\epsilon_0\hbar}\int d\Omega_k\sum_s|\hat{\boldsymbol{\mu}}\cdot\hat{\mathbf{e}}_{\mathbf{k}s}|^2e^{i\mathbf{k}\cdot(\mathbf{r}_i-\mathbf{r}_j)},$$

$$\Omega_{ij}=-\frac{\mu^2}{16\pi^2\epsilon_0\hbar}\int dk\,k^3\left[\frac{1}{k-k_0}+\frac{1}{k+k_0}\right]\times\int d\Omega_k\sum_s|\hat{\boldsymbol{\mu}}\cdot\hat{\mathbf{e}}_{\mathbf{k}s}|^2e^{i\mathbf{k}\cdot(\mathbf{r}_i-\mathbf{r}_j)},$$

with

$$\mathcal{N}'=\int_\Omega d\Omega_k\sum_s|\hat{\boldsymbol{\mu}}\cdot\hat{\mathbf{e}}_{\mathbf{k}s}|^2, \tag{21}$$

where $\hat{\boldsymbol{\mu}}$ is the unit vector along the transition electric dipole moment $\boldsymbol{\mu}$, and $\mu=|\boldsymbol{\mu}|$. In the derivation of Eqs. (20) and (21) we have assumed that the dipole moments of the atoms are parallel. This is not an essential feature since the dipole moments are induced by the electromagnetic field. For a permanent dipole moments configurations different from parallel are possible [29]. To carry out the integrations and the polarization sums in Eqs. (20) and (21) we can go over to a spherical representation in which

$$\int_\Omega d\Omega_k\equiv\int_0^\theta d\theta_k\sin\theta_k\int_0^{2\pi}d\varphi_k, \tag{22}$$

and the unit orthogonal polarization vectors $\hat{\mathbf{e}}_{\mathbf{k}1}$ and $\hat{\mathbf{e}}_{\mathbf{k}2}$ may be taken as [30]

$$\begin{aligned}\hat{\mathbf{e}}_{\mathbf{k}1}&=(-\cos\theta_k\cos\varphi_k,-\cos\theta_k\sin\varphi_k,\sin\theta_k),\\ \hat{\mathbf{e}}_{\mathbf{k}2}&=(\sin\varphi_k,-\cos\varphi_k,0).\end{aligned} \tag{23}$$

With a circular representation for the polarization vectors, i.e.,

$$\begin{aligned}\hat{\mathbf{e}}_{\mathbf{k}+}&=\frac{1}{\sqrt{2}}(\hat{\mathbf{e}}_{\mathbf{k}1}+i\hat{\mathbf{e}}_{\mathbf{k}2}),\\ \hat{\mathbf{e}}_{\mathbf{k}-}&=\frac{1}{\sqrt{2}}(\hat{\mathbf{e}}_{\mathbf{k}1}-i\hat{\mathbf{e}}_{\mathbf{k}2}),\end{aligned} \tag{24}$$

and dipole moments $\hat{\boldsymbol{\mu}}=\mp(1,\pm i,0)/\sqrt{2}$ for $\Delta m=\pm1$ transitions, Eqs. (20) and (21) after a change of integration variable ($u=\cos\theta_k$) lead to

$$\eta_{ij}=\gamma\frac{1}{\mathcal{N}'}(A_i+iB_i)(A_j+iB_j),$$

$$\beta_{ij}=\gamma\frac{1}{\mathcal{N}'}(A_i-iB_i)(A_j+iB_j),$$

$$\gamma_{ij}=\tfrac{3}{2}\gamma\left[[1-(\hat{\boldsymbol{\mu}}\cdot\hat{\mathbf{r}}_{ij})^2]\frac{\sin(k_0r_{ij})}{k_0r_{ij}}+[1-3(\hat{\boldsymbol{\mu}}\cdot\hat{\mathbf{r}}_{ij})^2]\left[\frac{\cos(k_0r_{ij})}{(k_0r_{ij})^2}-\frac{\sin(k_0r_{ij})}{(k_0r_{ij})^3}\right]\right], \tag{25}$$

$$\Omega_{ij}=\tfrac{3}{2}\gamma\left[-[1-(\hat{\boldsymbol{\mu}}\cdot\hat{\mathbf{r}}_{ij})^2]\frac{\cos(k_0r_{ij})}{k_0r_{ij}}+[1-3(\hat{\boldsymbol{\mu}}\cdot\hat{\mathbf{r}}_{ij})^2]\left[\frac{\sin(k_0r_{ij})}{(k_0r_{ij})^2}+\frac{\cos(k_0r_{ij})}{(k_0r_{ij})^3}\right]\right],$$

where $2\gamma=2\gamma_{ii}=k_0^3\mu^2/3\pi\epsilon_0\hbar$ is the Einstein A coefficient for spontaneous emission, $\hat{\mathbf{r}}_{ij}$ is the unit vector along the $\mathbf{r}_{ij}$, and

$$\begin{aligned}\mathcal{N}'&=\tfrac{1}{2}[1-\tfrac{1}{4}(\cos\theta)(3+\cos^2\theta)],\\ A_i&=\tfrac{3}{8}\int_{\cos\theta}^1du(1+u^2)\cos[k_0(r_z^{(i)}-r_z^{(s)})u]\times J_0(k_0r_x^{(i)}(1-u^2)^{1/2}),\\ B_i&=\tfrac{3}{8}\int_{\cos\theta}^1du(1+u^2)\sin[k_0(r_z^{(i)}-r_z^{(s)})u]\times J_0(k_0r_x^{(i)}(1-u^2)^{1/2}),\end{aligned} \tag{26}$$

with J_0 the zeroth-order Bessel function.

The coefficients γ_{ij} and Ω_{ij}, which appear in Eq. (25), are familiar in the theory of interaction between two identical two-level atoms [14,31]. They depend on the interatomic separation r_{ij} and describe collective properties of the two-atom system. For large interatomic separations k_0r_{ij} goes to infinity, and then γ_{ij} and Ω_{ij} go to zero, i.e., there is no coupling between the atoms. For the two-atom Dicke model, $k_0r_{ij}\ll1$, and then γ_{ij} reduces to γ, and Ω_{ij} reduces to the static dipole-dipole interaction potential which, for $k_0r_{ij}\to0$, tends to infinity.

The squeezed vacuum field introduces new decay coefficients η_{ij} and β_{ij} which are due to the coupling between the atoms and squeezed imperfect dipole wave. These parameters depend on the atom's position relatively to the point where the squeezed field is focused. Moreover, they depend on the angle θ over which the squeezed field is propagated. For small θ ($\theta\ll1$), A_i and B_i go to zero, and then there is not any effect of the squeezed vacuum field on the atoms. In this case, the atoms interact only with the ordinary vacuum modes. Otherwise, for large θ ($\theta\approx\pi$) most of the modes coupled to the atoms are squeezed, and then there is a strong effect of the squeezed field on the atoms. When $\theta=\pi$, all modes coupled to the atoms are squeezed, and then the atoms interact with the perfect squeezed dipole wave. In this case, there is not any spontaneous emission to the ordinary vacuum modes.

Now, we use the master equation (17) with the

coefficients (25) to calculate the population of the superradiant state $|+\rangle$. In this section we consider the two-atom Dicke model in which interatomic separations are much smaller than the resonant wavelength. Moreover, for simplicity, we choose the center of coordinates at the point where the squeezed field is focused, i.e., $r_z^{(s)}=0$. In this case, $r_x^{(1)}=r_x^{(2)}=r_x$, $r_z^{(1)}=r_z^{(2)}=r_z$, and then $A_1=A_2=A$ and $B_1=B_2=B$. The coefficients A and B now depend only on the coordinates r_x and r_z of the atoms. By varying r_x and r_z, we will be able to gauge the area over which the effect of the squeezed field on the atoms is important. We use the set of collective states $|1\rangle$, $|+\rangle$, and $|2\rangle$ as an appropriate representation for the density operator

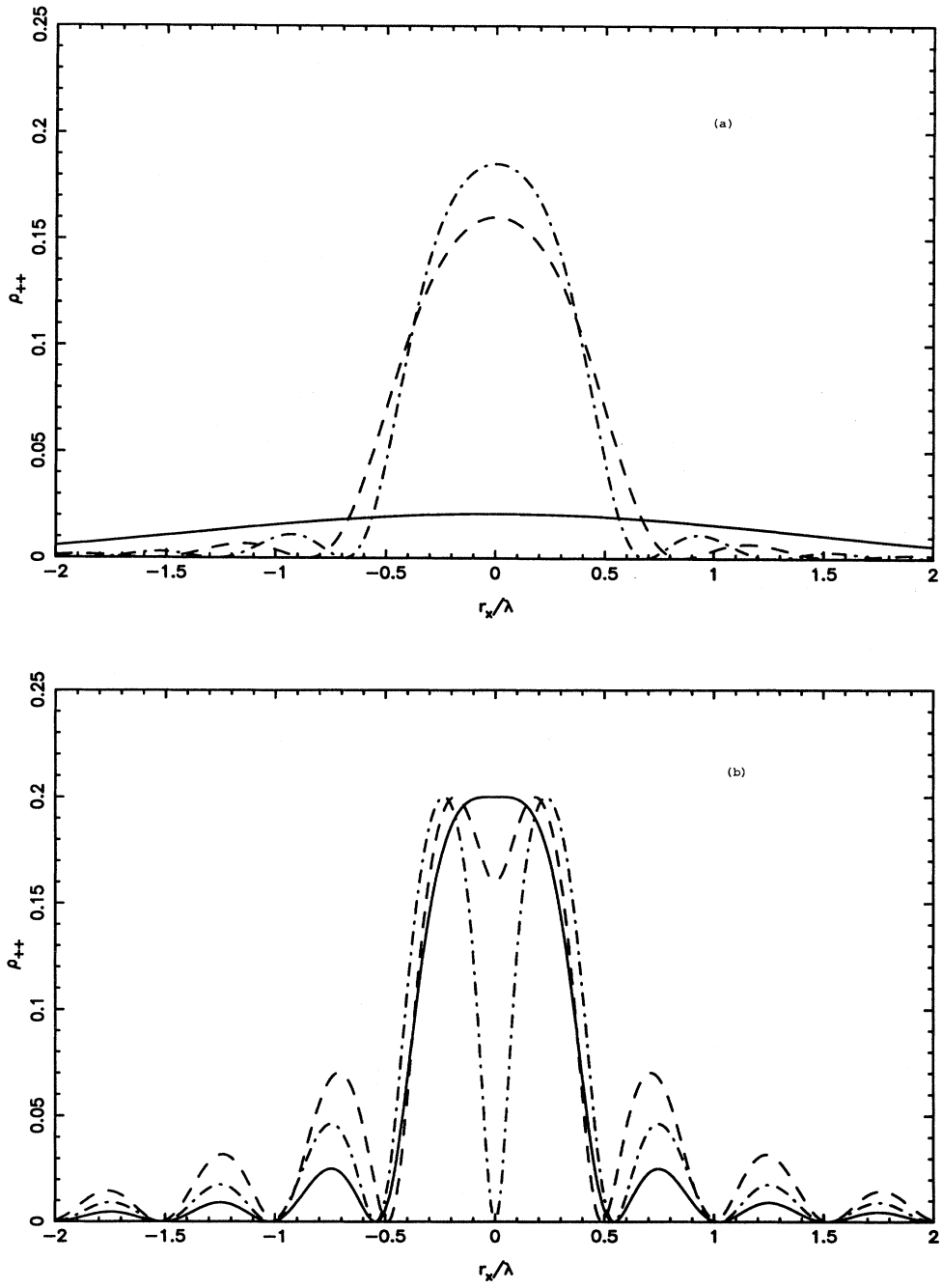

FIG. 2. Steady-state population of the state $|+\rangle$ as a function of r_x/λ for $r_z=0$, $N=2$, and different values of the angle θ over which squeezed field is propagated: (a) $\theta=10°$ (solid line), $\theta=45°$ (dashed line), $\theta=60°$ (dash-dotted line); and (b) $\theta=90°$ (solid line), $\theta=135°$ (dashed line), $\theta=180°$ (dash-dotted line).

$$\rho=\sum_{i,j}\rho_{ij}|i\rangle\langle j| , \tag{27}$$

where ρ_{ij} are the matrix elements of the reduced atomic density operator in the representation of the collective states. With the representation (27) the master equation (17) leads to the following, closed set of three equations of motion:

$$\begin{aligned}
\dot{\rho}_{22}&=-(n+1)\rho_{22}+(n-1)\rho_{++}+w|M|\rho_{\varphi} ,\\
\dot{\rho}_{++}&=(n-1)-(3n-1)\rho_{++}+2\rho_{22}-2w|M|\rho_{\varphi} ,\\
\dot{\rho}_{\varphi}&=2w|M|-n\rho_{\varphi}-6w|M|\rho_{++} ,
\end{aligned} \tag{28}$$

where $w=(A^2+B^2)/\mathcal{N}$, $n=(2wN+1)$, and

$$\rho_{\varphi}=[\rho_{21}\exp(-i\varphi_v)+\rho_{12}\exp(i\varphi_v)] .$$

By setting the left-hand side of Eqs. (28) equal to zero we obtain the steady-state solution of these equations. A straightforward algebraic manipulation of Eq. (28) leads to the following solution for the steady-state population of the superradiant state $|+\rangle$:

$$\rho_{++}=\frac{(n^2-1)-4w^2|M|^2}{(3n^2+1)-12w^2|M|^2} . \tag{29}$$

The steady-state solution (29), apart from the parameter N, also include the absolute value of the parameter M, which means that the squeezed vacuum field affects the steady-state population of the state $|+\rangle$. When the atoms interact with the thermal field, then $N\neq 0$, $|M|=0$, and the steady-state population of the state $|+\rangle$ is always different from zero. This means that with thermal field it is not possible to obtain pairwise atomic states in which the state $|+\rangle$ is unpopulated. If the atoms interact with the squeezed vacuum field, then $N\neq 0$, $|M|\neq 0$, and the steady-state population ρ_{++} can be reduced. For the minimum-uncertainty squeezed states, i.e., for $|M|^2=N(N+1)$, Eq. (29) reduces to

$$\rho_{++}=\frac{(n-1)(1-w)}{[3(n-1)(1-w)+2]} . \tag{30}$$

Since $0\leq w\leq 1$, the steady-state population in the state $|+\rangle$ can be reduced, and is equal to zero when $w=1$. This is illustrated on Fig. 2 where we have plotted the steady-state population of the state $|+\rangle$ given by Eq. (30) in function of the atomic distance r_x from the point where the squeezed field is focused, for $N=2$, $r_z=0$, and different angles θ over which the squeezed field is propagated. These graphs show that the population of the state $|+\rangle$ is strongly dependent on the angle θ over which squeezed field is propagated. As the angle θ increases from small values to $\theta=\pi/2$, the population of the state $|+\rangle$ increases [see Fig. 2(a)]. For angles θ larger than $\pi/2$, and $r_x\approx 0$, the population in the state $|+\rangle$ decreases with increasing θ, and is equal to zero for $\theta=\pi$, i.e., when the atoms interact with the perfect squeezed dipole wave. Figure 3 shows the steady-state population of the state $|+\rangle$ as a function of the atomic variations in the z direction for $N=2$, $r_x=0$, and different θ. It is seen that the population in the state $|+\rangle$ for the atomic variations in the z direction is slightly different from that for the variations in the x direction [see Fig. 2(b)]. The effect of squeezing can still be seen for sufficiently small r_z and the angles θ larger than $\pi/2$. The reduction of the population persists over as large an area in the z direction as in the x direction. The present

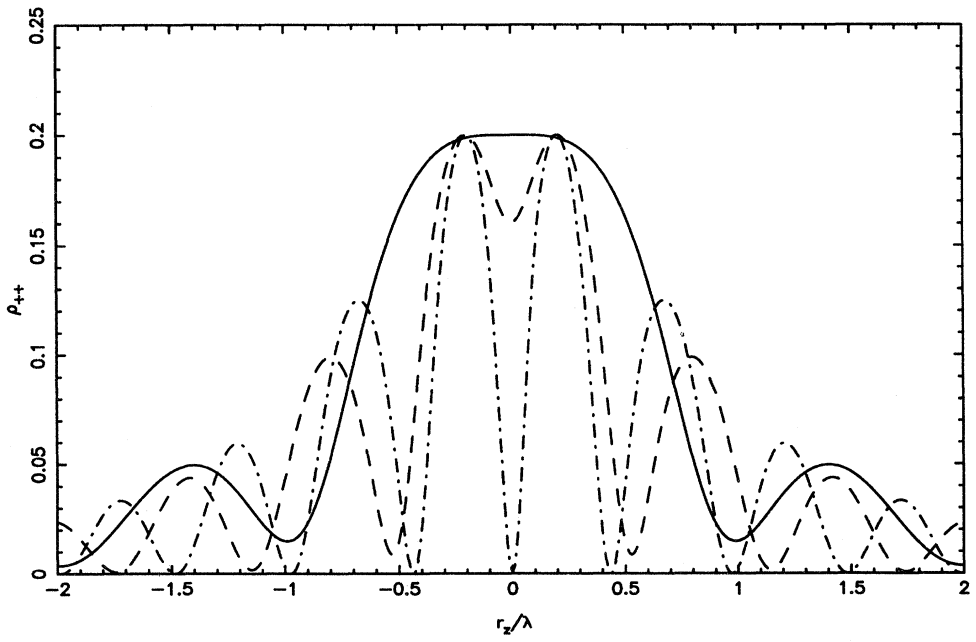

FIG. 3. Steady-state population of the state $|+\rangle$ as a function of r_z/λ for $r_x=0$, $N=2$, and different values of θ: $\theta=90°$ (solid line), $\theta=135°$ (dashed line), $\theta=180°$ (dash-dotted line).

results show that the reduction of the population in the state $|+\rangle$ is only possible when the squeezed field propagates over the angle θ greater than $\pi/2$. This means that the experiments in which the input squeezed field is directly incident on the atoms cannot be used to observe the pairwise atomic states. The production of a squeezed vacuum field incident on the atoms under the angles θ larger than $\pi/2$ will therefore be an important component of the experimental verification of this effect. This would evolve placing the atoms at the focal point of an appropriately large parabolic mirror. Other methods of producing near dipole wave would include recent experiments with atoms fixed in organic layers [32] or in crystals [33] and placed near a conducting metal surface. In light of these developments the experiment under discussion seems to be plausible.

IV. TWO ATOMS IN FREE SPACE WITH THE INTERATOMIC SEPARATION INCLUDED

In Sec. III we have assumed that the two-atom Dicke model interacts in free space with the squeezed vacuum field. In the Dicke model it is assumed that the interatomic separations are much smaller than the resonant wavelength, and all effects connected with the spatial distribution of the atoms are ignored. This assumption, however, may prove difficult in experimental realizations of such a model in free space. In atomic-beam experiments or atoms fixed in organic layers [32,33] the atomic separations are on the order of a resonant wavelength. Therefore it seems natural to study in some detail what happens when the atoms are separated by distances comparable to the resonant wavelength.

With the interatomic separation included, the antisymmetric state $|-\rangle$ cannot be decoupled from the symmetric states $|1\rangle$, $|+\rangle$, and $|2\rangle$. The presence of the antisymmetric state $|-\rangle$ may effect dynamics of our two-atom system. We limit the discussion to the case of variations in the atomic position along the x axis and we assume that $r_z^{(1)}=r_z^{(2)}=0$. By choosing the center of coordinates at the point where the squeezed field is focused, one finds from Eq. (17) that $A_1\neq A_2$ and $B_i=0$. Moreover, $\gamma_{ij}\neq\gamma$, and now the antisymmetric state $|-\rangle$ is coupled to the other symmetrical states (see Fig. 1). Using an appropriate representation (27) for the density operator with the antisymmetric state $|-\rangle$ included, the master equation (17), with the coefficients (25), leads to the following closed set of seven equation of motion, which can be written in matrix form as

$$\frac{d}{d\tau}\mathbf{X}=\underline{A}\mathbf{X}+\mathbf{I}\ , \tag{31}$$

where $\tau=2\gamma t$, $\mathbf{X}$ is a column vector with the real components

$$\begin{aligned}&X_1=\rho_{++},\quad X_2=\rho_{--}\ ,\\ &X_3=[\rho_{21}\exp(-i\phi_v)+\rho_{12}\exp(i\phi_v)]\ ,\\ &X_4=\rho_{22},\quad X_5=(\rho_{+-}+\rho_{-+}),\quad X_6=-i(\rho_{+-}-\rho_{-+})\ ,\\ &X_7=i[\rho_{21}\exp(-i\phi_v)-\rho_{12}\exp(i\phi_v)]\ ,\end{aligned} \tag{32}$$

and the inhomogeneous vector term $\mathbf{I}$ has the nonzero components

$$I_1=N_1,\quad I_2=N_2,\quad I_3=2\alpha|M|,\quad I_5=2uN\ . \tag{33}$$

In Eq. (31), $\underline{A}$ is the real 7×7 matrix

$$\underline{A}=\begin{pmatrix}(3N_1+1+a) & N_1 & M_1 & -(1+a) & 0 & 0 & 0\\ N_2 & (3N_2+1-a) & -M_2 & -(1-a) & 0 & 0 & 0\\ 2(M_1+\alpha|M|) & -2(M_2-\alpha|M|) & n & 0 & 0 & 0 & 0\\ -N_1 & -N_2 & -\alpha|M| & (n+1) & uN & 0 & 0\\ 2uN & 2uN & 0 & 4uN & n & b & 0\\ 0 & 0 & 0 & 0 & -b & n & -2u|M|\\ 0 & 0 & 0 & 0 & 0 & -2u|M| & n\end{pmatrix}\ . \tag{34}$$

For simplicity, in Eqs. (32)–(34) we have introduced the notation

$$\begin{aligned}&N_1=(w+\alpha)N,\quad N_2=(w-\alpha)N\ ,\\ &a=\gamma_{12}/\gamma,\quad b=\Omega_{12}/\gamma\ ,\\ &M_1=(w+\alpha)|M|,\quad M_2=(w-\alpha)|M|,\quad n=(2wN+1)\ ,\end{aligned} \tag{35}$$

with

$$\begin{aligned}&w=(A_1^2+A_2^2)/2\mathcal{N}',\quad u=(A_1^2-A_2^2)/2\mathcal{N}'\ ,\\ &\alpha=A_1A_2/\mathcal{N}'\ ,\end{aligned} \tag{36}$$

where A_1, A_2, and $\mathcal{N}'$ are defined in Eq. (26).

By setting the left-hand side of Eq. (31) equal to zero we obtain the steady-state solution of this equation. The steady-state solution of the X_1 component of the vector $\mathbf{X}$, which describes population in the superradiant state $|+\rangle$, is

$$X_1=\rho_{++}=\frac{\Phi_1\Phi_2+(a-2)\Phi_3-\Phi_4}{4(\Phi_1\Phi_2+a\Phi_3)}\ , \tag{37}$$

where

$$
\begin{aligned}
\Phi_1 &= \tfrac{1}{2}[(n^2-4u^2|M|^2)(n^2-4u^2N^2)+n^2b^2] , \\
\Phi_2 &= n[n^2-(2\alpha N+a)^2] \\
&\quad +2|M|^2[2\alpha w(2\alpha N+a)-n(\alpha^2+w^2)] , \\
\Phi_3 &= n(n^2+b^2-4u^2|M|^2) \\
&\quad \times[nN(wa-\alpha)+2\alpha(w-\alpha a)|M|^2] , \\
\Phi_4 &= \tfrac{1}{2}n(n^2+b^2-4u^2|M|^2) \\
&\quad \times[2(wa-\alpha)(nN-2w|M|^2)+n(1-a^2)] .
\end{aligned} \tag{38}
$$

The steady-state solution (37), apart from the squeezing parameters N and $|M|$, depends also on the interatomic interaction parameters γ_{12} and Ω_{12}. Figure 4 shows the stationary populations ρ_{++} as a function of $r_x=(r_x^{(1)}+r_x^{(2)})/2$, which is the center of the interatomic axis, for $N=2$, the squeezed field incidents over the angle $\theta=\pi$, and different interatomic separations r_{12}. It is seen that the steady-state population of the state $|+\rangle$ strongly depends on the interatomic separation. For $|r_x|<\lambda/2$ the stationary population ρ_{++} decreases with decreasing of the interatomic separation r_{12} and is equal to zero for very small r_{12}. However, in this case equal to zero population in the state $|+\rangle$ does not mean that the system is in the pairwise atomic state. This is due to the presence of the antisymmetric state $|-\rangle$, which has a population different from zero for small interatomic separations. It is not difficult to show from Eqs. (31)–(36) that in the steady state the population in the antisymmetric state $|-\rangle$ is

$$
\rho_{--}=\frac{\Phi_1\Phi_2+(a+2)\Phi_3-\Phi_4}{4(\Phi_1\Phi_2+a\Phi_3)} . \tag{39}
$$

Figure 5 illustrates the effect of the interatomic separation on the population in the state $|-\rangle$. It is seen that the population in the state $|-\rangle$ for $|r_x|<\lambda/2$ is always different from zero and increases when r_{12} decreases. Since the antisymmetric state $|-\rangle$ is populated the system is not in the pairwise atomic state.

It should be emphasized here that in the limit of small r_{12} the steady state of the system, with the interatomic separation included, does not reduce to that of the Dicke model. This fact is connected with conservation of S^2 for the Dicke model and S^2 not being a constant of motion for the system with the interatomic separation included [34]. To explain it we express the square of the total spin of the two-atom system in terms of the density matrix elements as

$$
S^2=2-2\rho_{--} . \tag{40}
$$

It is evident from Eq. (40) that S^2 is conserved only in the Dicke model, in which the antisymmetric state $|-\rangle$ is ignored. For a system with the interatomic separation included the antisymmetric state is populated and S^2 is not conserved. This state is populated even for small interatomic separations ($a\rightarrow 1$). The Dicke system reaches steady state between the triplet states $|1\rangle$, $|+\rangle$, and $|2\rangle$. The singlet state $|-\rangle$ remains unpopulated. The S^2

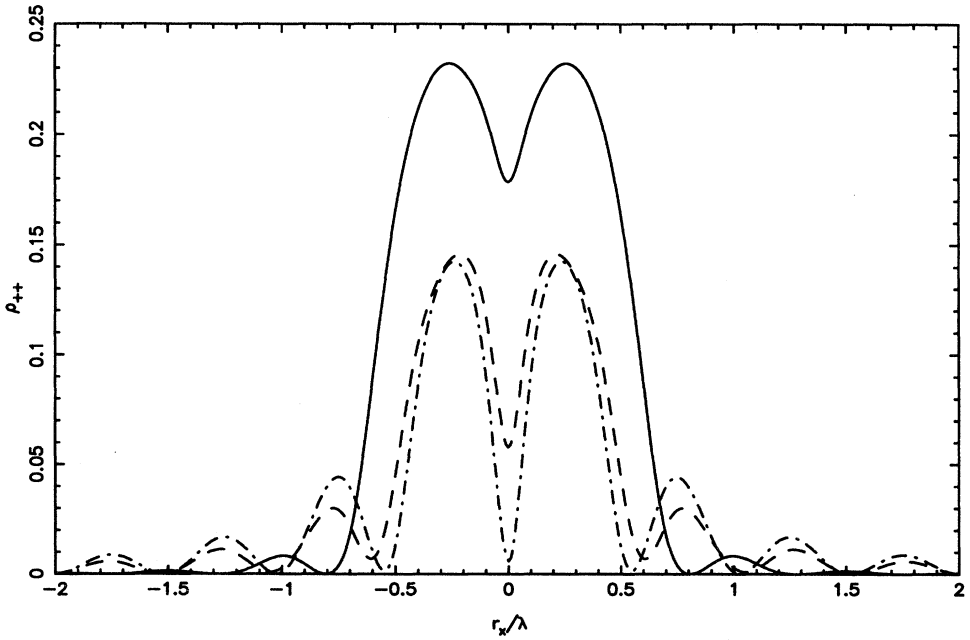

FIG. 4. Steady-state population of the state $|+\rangle$ as a function of r_x/λ for $N=2$, $\theta=180°$, and different interatomic separations: $r_{12}=\lambda/2$ (solid line), $r_{12}=\lambda/4$ (dashed line), $r_{12}=\lambda/12$ (dash-dotted line).

breaking system reaches steady state between all triplet and singlet states. With Eq. (39), and in the strong field limit ($N \gg 1$), Eq. (40) takes the value $\frac{3}{2}$, independent of the interatomic separation r_{12}. This value signifies the same population of all triplet and singlet states of the system.

We can, however, employ the S^2 breaking system to create the pairwise atomic state. This could be achieved assuming that the observation time is shorter than $(2\gamma)^{-1}$. The singlet state $|-\rangle$ decays on a time scale $\sim[2(\gamma-\gamma_{12})]^{-1}$, which for $\gamma_{12}\approx\gamma$ is much longer than $(2\gamma)^{-1}$ (see Fig. 1). However, this time must be small compared to observation times in order that the steady state (39) be reached, with the singlet state participating fully in the interaction. On the other hand, the superradiant state $|+\rangle$ decays on a time scale $\sim[2(\gamma+\gamma_{12})]^{-1}$, which for small interatomic separations is shorter than $(2\gamma)^{-1}$. Clearly, as we consider short observation times [order $(2\gamma)^{-1}$], the singlet state does not participate in the interaction and the system reaches the steady state only between the triplet states. For times of order $(2\gamma)^{-1}$ and for small interatomic separations, only the ground state $|1\rangle$ and the most excited state $|2\rangle$ are populated, and the steady state behaves as the pairwise atomic state.

In conclusion, with the interatomic separation included the steady state of two atoms interacting with a perfect squeezed dipole wave is not the pairwise atomic state. This is due to the presence of the antisymmetric state $|-\rangle$ when the interatomic separations are included. This state shows a large steady-state population in contrast to the superradiant state $|+\rangle$, which is not populated for small interatomic separations. This system, however, can be in the pairwise atomic state providing that interatomic separations are small and the observation time is shorter than $(2\gamma)^{-1}$. For observation times larger than $(2\gamma)^{-1}$ the system is not in the pairwise atomic state even for small interatomic separations. In this case the effect of squeezed vacuum field is manifested by the selective population of collective atomic states. This is a novel effect, which does not appear in the thermal as well as in ordinary vacuum field. The experiments discussed in Sec. III are fully applicable to this model. Since the antisymmetric state $|-\rangle$ does not radiate in the direction perpendicular to the atomic axes [14,31], a detector located in this direction will observe only the population of the state $|+\rangle$.

V. EFFECT OF A MICROSCOPIC FABRY-PÉROT CAVITY

The interaction of the squeezed vacuum field with the two-atom system leads to the selective population of the collective atomic states. In free space the two-atom Dicke model can decay to a pure state in which only the ground state $|1\rangle$ and the state $|2\rangle$ are excited. The two-atom system with the interatomic separations included always decays to a mixed state in which the superradiant state $|+\rangle$ is not populated only for small interatomic separations. These effects are sensitive to the angle θ over which the squeezed vacuum field is propagated and in free space can be observed when more than 50% modes coupled to the atoms is squeezed. The production of a squeezed wave incident on the atoms over a large angle θ will therefore be an important component of the ex-

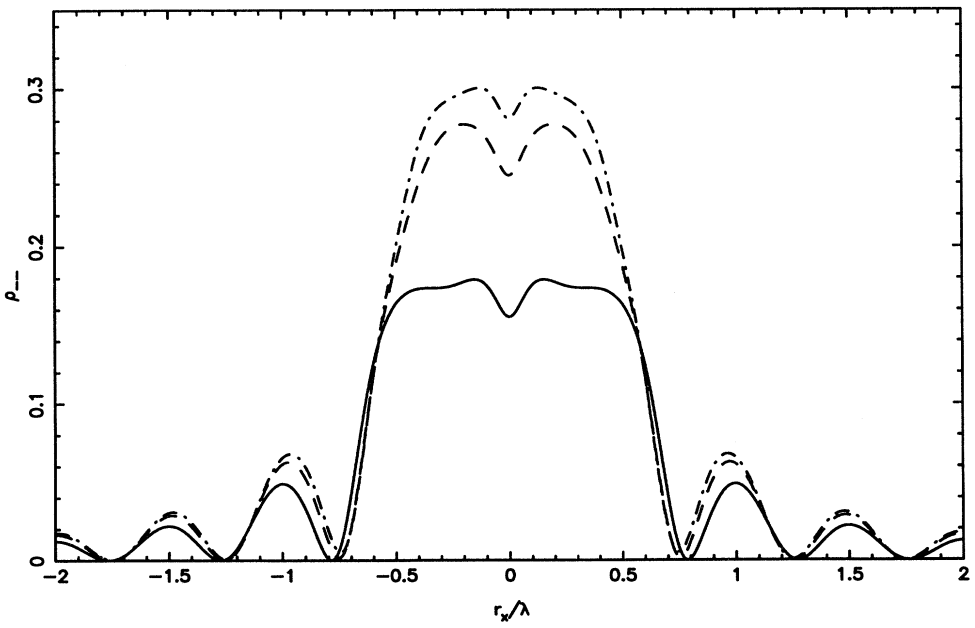

FIG. 5. Same as in Fig. 4 but for the antisymmetric state $|-\rangle$.

perimental verification of these effects. To avoid this we shall examine the interaction of the squeezed vacuum field with the atoms located inside a microscopic Fabry-Pérot cavity. Inside the cavity, a strong selection of radiation modes coupling to atoms is possible [17] and only the modes whose propagation vectors lie within a small solid angle about a line perpendicular to the mirror surfaces are coupled to the atoms. Recently, Parkins and Gardiner [2] have applied this model to the inhibition of atomic phase decays by squeezed light. They have demonstrated that a significant reduction in fluctuations experienced by the atom can be achieved in one quadrature even for a small angle θ over which the squeezed light is propagated. Here we examine the pairwise atomic states in the two-atom Dicke model located inside the microscopic Fabry-Pérot cavity. Our treatment is based on the quantum theory of spontaneous emission from the microscopic Fabry-Pérot cavity recently developed by DeMartini *et al.* [35].

Assume that we have the plane-mirror Fabry-Pérot configuration (Fig. 6) with two mirrors which lie parallel to the xy plane. The first is a perfectly reflecting mirror located at $z=0$, and the second a partially transmitting lossless mirror is located at $z=L$. The partially transmitting mirror has a real reflectivity R and transmittivity $i(1-R^2)^{1/2}$—the same for both directions. We assume that the mirrors are very large, so that end effects can be ignored.

By a consideration of boundary conditions at the mirrors [35,36], we derive the following expression for the mode function $\mathbf{g}_{\mathbf{k}s}(\mathbf{r})$ inside the cavity:

$$\mathbf{g}_{\mathbf{k}s}(\mathbf{r})=\left[\frac{ck}{2\epsilon_0\hbar(2\pi)^3}\right]^{1/2} Y(\theta_k,L)(\hat{\mathbf{e}}_{\mathbf{k}s}e^{i\mathbf{k}\cdot\mathbf{r}}+\hat{\mathbf{e}}'_{\mathbf{k}s}e^{i\mathbf{k}'\cdot\mathbf{r}}) , \tag{41}$$

where $Y(\theta_k,L)$ is the cavity transfer function

$$Y(\theta_k,L)=\frac{i(1-R^2)^{1/2}}{1-R\exp[-2ikL\cos\theta_k]} , \tag{42}$$

with θ_k the angle between the $\mathbf{k}$ vector and the cavity axis. We have assumed that the reflectivity R is the same for both polarizations. The polarization vectors $\hat{\mathbf{e}}_{\mathbf{k}s}$ and $\hat{\mathbf{e}}'_{\mathbf{k}s}$ can be written as a sum of components parallel and perpendicular to the xy plane as

$$\hat{\mathbf{e}}_{\mathbf{k}s}=\hat{\mathbf{e}}^{\perp}_{\mathbf{k}s}+\hat{\mathbf{e}}^{\parallel}_{\mathbf{k}s},\quad \hat{\mathbf{e}}'_{\mathbf{k}s}=\hat{\mathbf{e}}^{\perp}_{\mathbf{k}s}-\hat{\mathbf{e}}^{\parallel}_{\mathbf{k}s} , \tag{43}$$

and similarly for the wave vectors $\mathbf{k}$ and $\mathbf{k}'$

$$\mathbf{k}=\mathbf{k}^{\perp}+\mathbf{k}^{\parallel},\quad \mathbf{k}'=-\mathbf{k}^{\perp}+\mathbf{k}^{\parallel} . \tag{44}$$

The mode function (41) for the cavity is modified, compared to that for free space (19), by the presence of mirrors which is manifested by the function $Y(\theta_k,L)$. The effect of $Y(\theta_k,L)$ is most clearly exhibited in the form

$$|Y(\theta_k,L)|^2=\frac{(1-R^2)}{(1-R)^2+4R\sin^2(kL\cos\theta_k)} , \tag{45}$$

which is identified as the Airy function of the cavity [37]. If R is close to 1, then this function displays a series of sharp peaks for angles of incidence such that $\sin(kL\cos\theta_k)=0$. If $L=\lambda/2$, the function (45) will exhibit a peak centered at $\cos\theta_k=1$. It means that a strong coupling is affected only with those modes which are contained in a small solid angle centered at z axis. In our model the two-atom Dicke system is coupled to these modes, part of which can be squeezed by input squeezed field. To maximize the coupling between the atoms and squeezed input field we assume perfect matching between the input squeezed modes and the cavity modes. Later we shall examine imperfect matching, where we shall match a focused Gaussian beam with the cavity modes.

With the mode functions (5) and (41), and on using (22)–(24) and (43)–(45), the decay constants and the dipole-dipole interaction term in Eq. (18) take the following form:

$$\begin{aligned}
\eta_{ij}&=\frac{3}{2}\gamma\frac{(1+R)}{(1-R)}\frac{1}{\mathcal{N}'}\left[\int_{\cos\theta}^{1}du(1+u^2)\frac{\sin^2(k_0r_zu)}{1+F\sin^2(k_0Lu)}\right.\\
&\qquad\left.\times J_0(k_0r_x(1-u^2)^{1/2})\right]^2 ,\\
\beta_{ij}&=\frac{3}{2}\gamma\frac{(1+R)}{(1-R)}\frac{1}{\mathcal{N}'}\left|\int_{\cos\theta}^{1}du(1+u^2)\frac{\sin^2(k_0r_zu)}{1+F\sin^2(k_0Lu)}\right.\\
&\qquad\left.\times J_0(k_0r_x(1-u^2)^{1/2})\right|^2 ,\\
\gamma_{ij}&=\frac{3}{2}\gamma\frac{(1+R)}{(1-R)}\left[\int_{0}^{1}du(1+u^2)\frac{\sin^2(k_0r_zu)}{1+F\sin^2(k_0Lu)}\right] ,\\
\Omega_{ij}&=-\frac{\mu^2}{4\pi\epsilon_0\hbar}\frac{(1+R)}{(1-R)}\int dk\,k^3\left[\frac{2k}{k^2-k_0^2}\right]\\
&\qquad\times\int_0^1du(1+u^2)\frac{\sin^2(kr_zu)}{1+F\sin^2(kLu)}\\
&\qquad\times J_0(kr_{ij}(1-u^2)^{1/2}) ,
\end{aligned} \tag{46}$$

where now

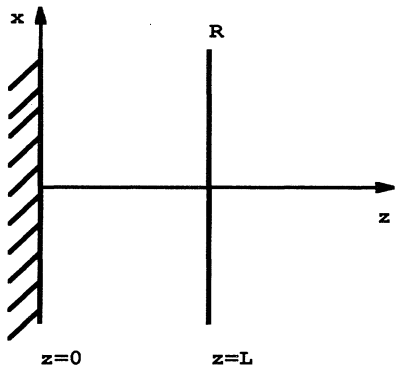

FIG. 6. Geometry of the microscopic Fabry-Pérot cavity. The left mirror is perfectly reflecting.

$$\mathcal{N}'=\int_{\cos\theta}^{1} du(1+u^2)\frac{\sin^2(k_0 r_z u)}{1+F\sin^2(k_0 L u)} , \tag{47}$$

and $F=4R/(1-R)^2$.

In derivation of Eqs. (46) and (47) we have assumed that the squeezed vacuum field is focused at $\mathbf{r}_0=(0,0,r_z)$, and the two-atom Dicke system is located at $\mathbf{r}=(r_x,0,r_z)$. The parameters (46) and (47) differ considerably from that for free space. In the limit $R\rightarrow 1$, with $r_z=L/2$ and $L=\lambda/2$, the parameter γ_{ij} approaches 1.5γ, which is in agreement with the result found by Milonni and Knight [38] and experimental testing by Hulet, Hilfer, and Kleppner [39]. This result shows that the spontaneous-emission rate is three times greater than the free-space rate when the atoms are between plane parallel perfect mirrors separated by half a wavelength.

The master equation (17), with the parameters (46) and (47), leads to the equation of motion for the density-matrix elements similar in form to the free-space equations (28), but now the parameters n and w are

$$n=(2wN+D), \quad w=A_{\rm cav}^2/\mathcal{N}' , \tag{48}$$

where $A_{\rm cav}=\eta_{ij}/\gamma=\beta_{ij}/\gamma$ and $D=\gamma_{ij}/\gamma$.

These new parameters reflect the effect of the cavity on the interaction between the squeezed vacuum field and the Dicke system. Replacing n and w in Eq. (28) by the parameters (48), and for minimum-uncertainty squeezed states, Eq. (28) leads to the following steady-state population of the state $|+\rangle$:

$$\rho_{++}=\frac{(n-D)(D-w)}{3(n-D)(D-w)+2D^2} . \tag{49}$$

Equation (49) is the exact formula describing the steady-state population of the superradiant state $|+\rangle$, valid for any values of the intensity of the squeezed field and the angles over which the squeezing is propagated as well as for different parameters of the cavity. This formula is illustrated graphically in Fig. 7 as a function of r_x/L for $R=0.99$, $r_z=0.5L$, $L=\lambda/2$, $N=2$, and for different values of the angle θ over which the squeezed field is propagated. These graphs show that a pronounced reduction of the population in the state $|+\rangle$ can be obtained even for small angles θ over which the squeezed field is propagated. The complete reduction of the population can be achieved for $\theta>20°$ at $r_x/L=0$, i.e., when the atoms are at the point where squeezed field is focused. In other words, the pairwise atomic states can be observed even when the atoms interact with an imperfect squeezed dipole wave. As one can see from Fig. 7, at $r_x/L=0$ there is relatively little variation in population for θ larger than 10°. This reflects the fact that inside the cavity the atoms are coupled only to these modes which are nearly perpendicular to the mirrors.

It is important to consider also the sensitivity of the effects to small changes in the mirror spacing L. This will be very pertinent to any practical experimental arrangement as the distances involved are extremely small. For $L<\lambda/2$, the mode density inside the cavity is greatly diminished, and we enter the regime of inhibited spontaneous emission [17,39]. Figure 8 illustrates the population in the state $|+\rangle$ for the same parameters as in Fig. 7, but with $L=0.49\lambda$. The population is still considerably reduced for sufficiently small r_x/L, however, the maximum relative reduction at $r_x/L=0$ is less than that

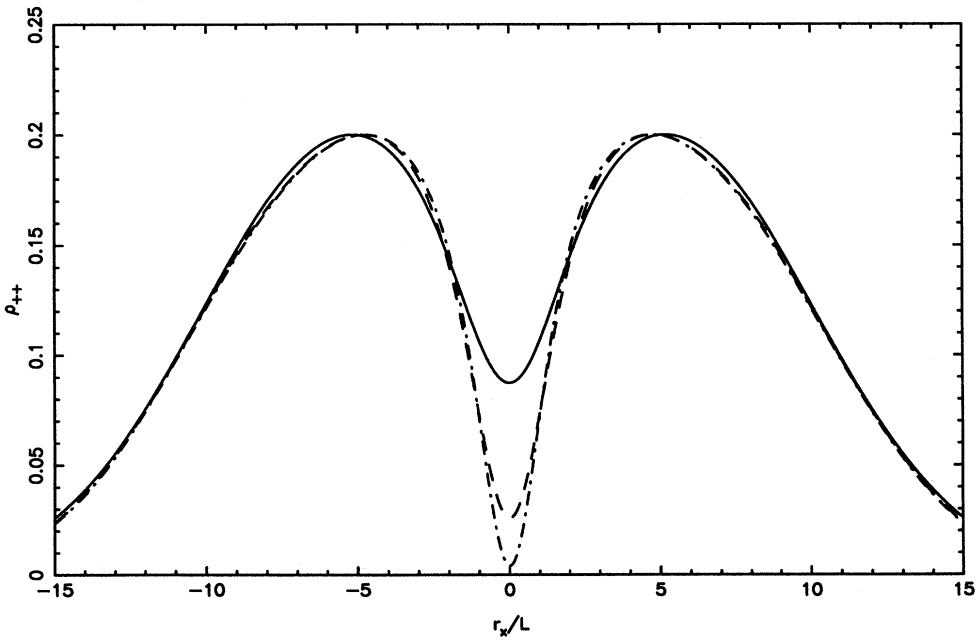

FIG. 7. Steady-state population of the state $|+\rangle$ as a function of r_x/L for $R=0.99$, $r_z=0.5L$, $L=\lambda/2$, $N=2$, and for different values of the angle θ: $\theta=5°$ (solid line), $\theta=10°$ (dashed line), $\theta=20°$ (dash-dotted line).

obtained with the same parameters for $L=\lambda/2$. Moreover, in the x direction the area over which significant reduction of the population occurs is considerably reduced in comparison to that for $L=\lambda/2$. Figure 9 illustrates the population in the state $|+\rangle$ for the same parameters as in Fig. 7, but for L slightly greater than $\lambda/2$. In this case ρ_{++} shows pronounced oscillations in the x direction. This occurs due to the greater number of modes available for coupling when L is larger than $\lambda/2$. The reduction of the population does not persist over as large an area as for $L=\lambda/2$, but the advantage now is that the magnitude of the reduction at $r_x/L=0$ is not changed, and we can still observe the pairwise atomic states.

In conclusion, by use of the microscopic cavity with $L=\lambda/2$, the pairwise atomic states can be produced by an imperfect squeezed dipole wave. It happens for small angles θ ($\theta>20°$), over which the squeezed field is propagated. There appears to be a reasonable range over which L may be varied and yet allow the pairwise atomic states. This range is biased towards values of L equal to or slightly larger than $\lambda/2$, as opposed to values of L less than $\lambda/2$, where this effect is slightly reduced.

VI. EFFECTS OF IMPERFECT MATCHING

In this section, we investigate the effect of imperfect matching between the cavity modes and the input squeezed modes on the steady-state population of the state $|+\rangle$. In practice, a perfectly matched input may not be possible, so it is important to repeat our calculations with the input mode function $U_s(\mathbf{k})$ given not by Eq. (5), but rather by some approximation to that function. We choose a Gaussian profile for the input squeezed field as an example of an approximate match. It is reasonable to expect that in the experimental setup a system of lenses will produce a focused squeezed field in a form of Gaussian beam. Since the atoms inside the cavity are coupled only to those modes which are nearly perpendicular to the mirrors we can use the paraxial approximation for a focused Gaussian beam [40]. In this approximation, the mode function $U_s(\mathbf{k})$, for $\theta_k<\theta$, can be written as

$$U_s(\mathbf{k})=\mathcal{N}_G^{-1/2}\boldsymbol{\mu}^*\cdot\mathbf{f}_{ks}^*(\mathbf{r}_0)\times\exp[-\delta\sin^2\theta_k-i(\eta-\varphi\sin^2\theta_k)]\ , \tag{50}$$

where

$$\mathbf{f}_{ks}(\mathbf{r}_0)=\left[\frac{ck}{2\epsilon_0\hbar(2\pi)^3}\right]^{1/2}(\hat{\mathbf{e}}_{ks}e^{i\mathbf{k}\cdot\mathbf{r}_0}+\hat{\mathbf{e}}'_{ks}e^{i\mathbf{k}'\cdot\mathbf{r}_0})\ , \tag{51}$$

and $\mathcal{N}_G$ is the normalization constant.

The parameters δ, η, and φ, which appear in Eq. (50), characterize the input Gaussian beam in the paraxial approximation. The parameter δ represents the beam spot size, φ represents the radius of curvature of the wave fronts, and η is the phase shift between this beam and the idealized plane wave.

Using the expression (50) and $U_s(\mathbf{k})$, and (41) for $\mathbf{g}_{ks}(\mathbf{r})$, with (22)–(24) and (43)–(45), the damping

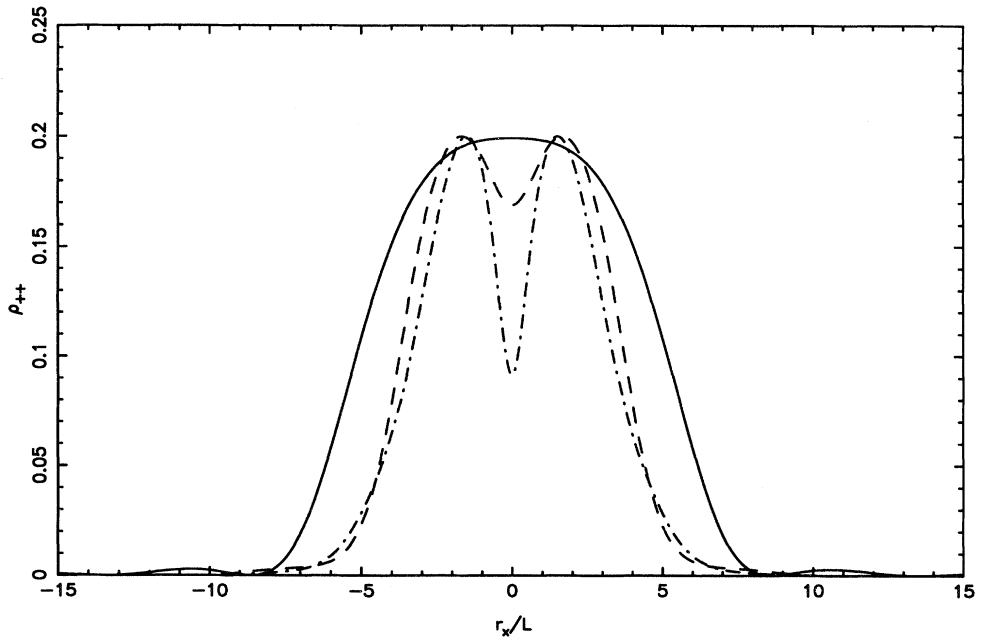

FIG. 8. Same as in Fig. 7 but for $L=0.49\lambda$.

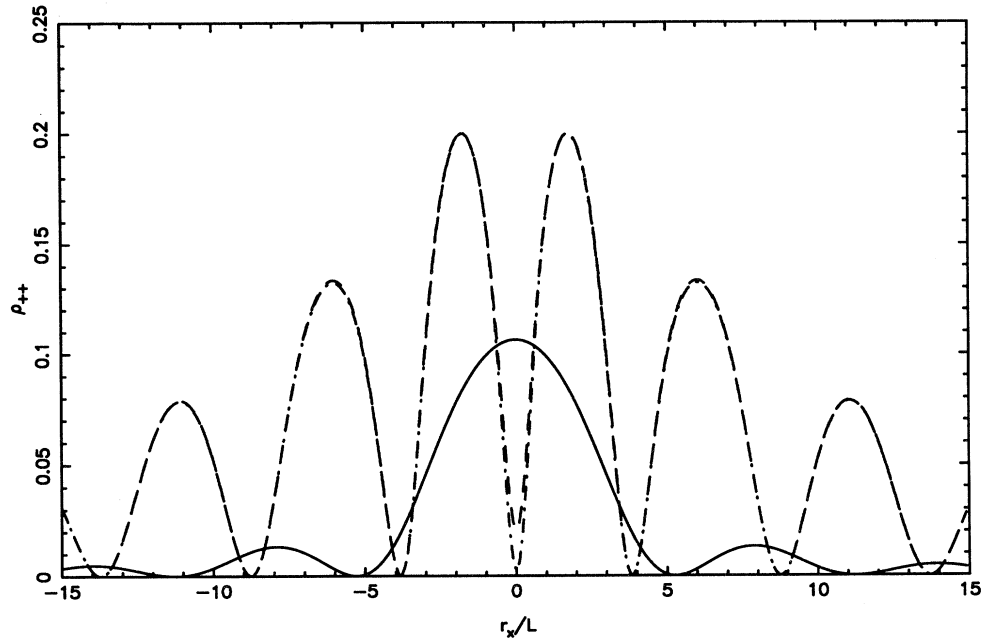

FIG. 9. Same as in Fig. 7 but for $L=0.51\lambda$.

coefficients η_{ij} and β_{ij} take the form

$$\eta_{ij}=\frac{3}{2}\gamma\frac{(1+R)}{(1-R)}\frac{e^{-2i\eta}}{\mathcal{N}_G}(G-iH)^2 , \tag{52}$$

$$\beta_{ij}=\frac{3}{2}\gamma\frac{(1+R)}{(1-R)}\frac{1}{\mathcal{N}_G}(G^2+H^2) , \tag{53}$$

where

$$G=\int_{\cos\theta}^{1}du(1+u^2)\frac{\sin^2(k_0r_zu)}{(1-R)[1+F\sin^2(k_0Lu)]}\times\{\cos[\varphi(1-u^2)]-R\cos[2k_0Lu-\varphi(1-u^2)]\}\times e^{-\delta(1-u^2)}J_0(k_0r_x(1-u^2)^{1/2}) , \tag{54}$$

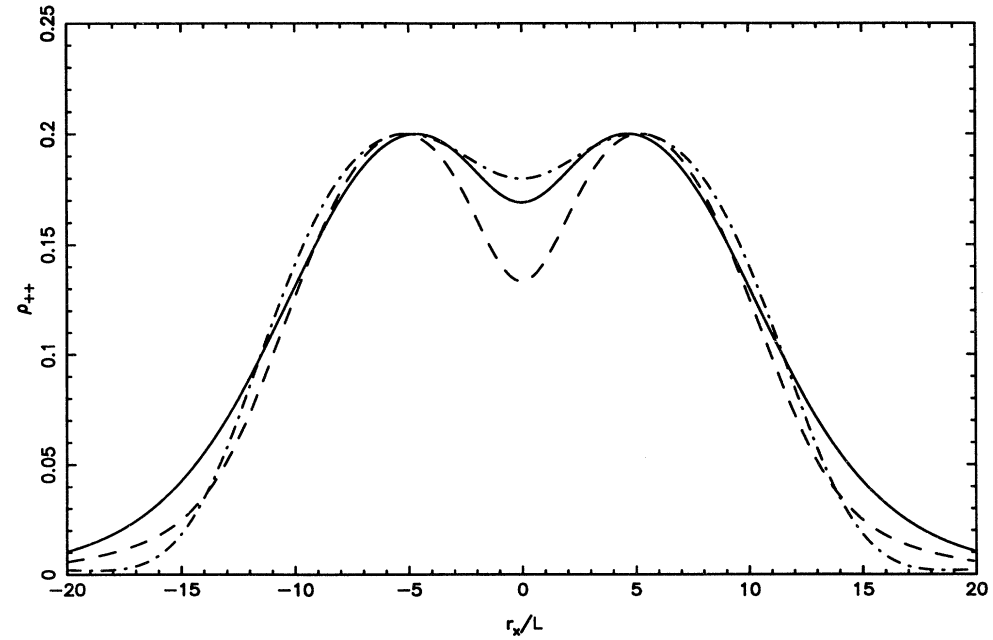

FIG. 10. Steady-state population of the state $|+\rangle$ as a function of r_x/L for the imperfect matching with $\delta=120$, $\eta=-\pi/2$, $R=0.99$, $\theta=5°$, $r_z=L/2$, $L=\lambda/2$, $N=2$, and different values of φ: $\varphi=0$ (solid line), $\varphi=100$ (dashed line), $\varphi=200$ (dash-dotted line).

$$H=\int_{\cos\theta}^{1} du \frac{(1+u^2)\sin^2(k_0 r_z u)}{(1-R)[1+F\sin^2(k_0 L u)]} \times\{\sin[\varphi(1-u^2)]+R\sin[2k_0 L u-\varphi(1-u^2)]\} \times e^{-\delta(1-u^2)} J_0(k_0 r_x (1-u^2)^{1/2}) , \quad (55)$$

and

$$\mathcal{N}_G=\int_{\cos\theta}^{1} du(1+u^2)e^{-2\delta(1-u^2)}\sin^2(k_0 r_z u) . \quad (56)$$

We note that the remain parameters γ_{ij} and Ω_{ij}, which appear in the master equation (17), are not altered by the Gaussian profile of the input beam, and are the same as in Eq. (46).

With the parameters (52) and (53), the master equation (17) leads to the steady-state population of the state $|+\rangle$, which is the same as for the perfect matching [Eq. (49)], but with the parameter w replaced by

$$w=\frac{1}{\mathcal{N}_G}(G^2+H^2) , \quad (57)$$

where G,H, and $\mathcal{N}_G$ are given by Eqs. (54)–(56).

Figure 10 shows the population in the state $|+\rangle$ as a function of r_x/L, for $R=0.99$, $\theta=5°$, $r_z=L/2$, $N=2$, $\delta=120$, $\eta=-\pi/2$, and different φ. These graphs show that with the Gaussian profile of the input squeezed field the population in the state $|+\rangle$ is always different from zero, but still can be significantly reduced around $r_x/L=0$. The magnitude of reduction strongly depends on the choice of φ, emphasizing the need for good matching of the mode functions. Reduced populations at $r_x/L=0$ are found for values of φ in range 0–200. Figure 10 shows that the reduction of the population is strongly dependent on φ. This effect is also sensitive to variations in δ, as we demonstrate in Fig. 11, where we fix $\varphi=80$, and compare results for different δ. Reduced populations at $r_x/L=0$ are found for values of δ in range 50–300. Figures 10 and 11 show that the area in the r_x direction, over which the populations are reduced is slightly changed in comparison to that for the perfect matching (see Fig. 7).

In conclusion, the imperfect matching between the input squeezed modes and the cavity modes has a destructive effect on the pairwise atomic states. Despite this, for a large range of the parameters characterizing a Gaussian profile of the input beam, it is still possible to obtain a significant reduction of the population of the state $|+\rangle$.

VII. SUMMARY

We have studied here the problem of interaction between a two-atom system and a three-dimensional squeezed vacuum field. We have been especially concerned with the steady-state solution for the population of the superradiant state $|+\rangle$, when (a) the two-atom Dicke system is in free space, (b) the two-atom system is in free space with the interatomic separation included, and (c) the two-atom Dicke system inside the microscopic cavity interacts with an imperfect squeezed dipole wave. In case (a) the population of the state $|+\rangle$ depends on the angle θ over which the squeezed field is propagated, and for small θ increases with increasing θ. For θ greater than $\pi/2$ the population decreases with increasing θ and is equal to zero for $\theta=\pi$, i.e., when the atoms interact

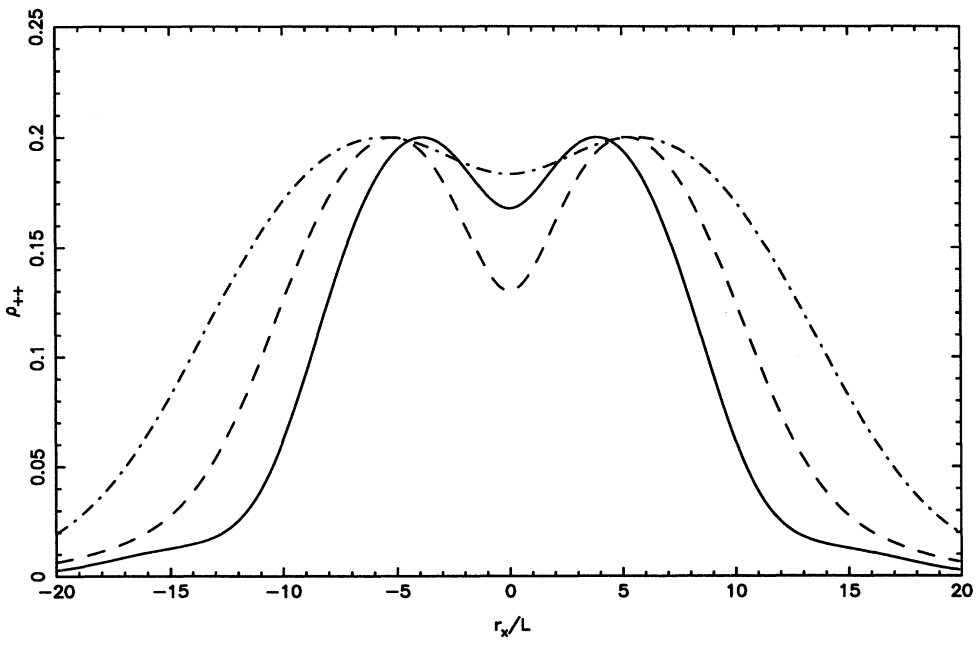

FIG. 11. Same as in Fig. 10 but for fixed $\varphi=80$ and different values of δ: $\delta=50$ (solid line), $\delta=120$ (dashed line), $\delta=300$ (dash-dotted line).

with a perfect dipole wave. In this case the two-atom Dicke system is in the pairwise atomic state in which both atoms are in their excited states or in their ground states. Case (b) exhibits features completely different from (a) in that the two-atom system with the interatomic separation includes decays to a state that is not the pairwise atomic state. This is due to the presence of the antisymmetric state $|-\rangle$ when the interatomic separation is included. However, the effect of squeezed field on the two-atom system is still evident and is manifested by the selective population of the collective atomic states. In case (c) the population in the state $|+\rangle$, unlike the free-space case, can be reduced to zero at a small angle θ over which the squeezed field is propagated. However, this is sensitive to the mode matching between the input squeezed field and the cavity, and occurs only when the input squeezed modes are perfectly matched to the cavity modes. For an imperfect matching, as with a Gaussian profile for the input beam, the effect of the squeezed field is less evident, but still we observe a significant reduction of the population in the state $|+\rangle$.

The present analysis of pairwise atomic states show that this effect is sensitive to the angle of propagation of the squeezed field. If the experiment were prepared with the atoms in free space, the production of a squeezed electric dipole wave will be an important component for the verification of this effect. Our results show that this can be avoided by using the microscopic Fabry-Pérot cavity. Experiments with the optical microscopic cavity have been performed recently [35] and, as we have shown here, can be applied to observation of the pairwise atomic states.

ACKNOWLEDGMENTS

I would like to thank P. D. Drummond for suggesting an investigation of this problem, and S. M. Barnett and B. J. Dalton for some illuminating discussions.

*On leave from Institute of Physics, Adam Mickiewicz University, Poznań, Poland.

[1] C. W. Gardiner, Phys. Rev. Lett. **56**, 1917 (1986).
[2] A. S. Parkins and C. W. Gardiner, Phys. Rev. A **40**, 3796 (1989); **42**, 5765(E) (1990).
[3] M. A. Marte, H. Ritsch, and D. F. Walls, Phys. Rev. A **34**, 3577 (1988).
[4] H. J. Carmichael, A. S. Lane, and D. F. Walls, Phys. Rev. Lett. **58**, 2539 (1987); H. Ritsch and P. Zoller, Phys. Rev. A **38**, 4657 (1988); A. S. Parkins, *ibid.* **42**, 4352 (1990).
[5] J. Gea-Banacloche, Phys. Rev. Lett. **62**, 1603 (1989); J. Javanainen and P. L. Gould, Phys. Rev. A **41**, 5088 (1990).
[6] Z. Ficek and P. D. Drummond, Phys. Rev. A **43**, 6247 (1991); **43**, 6258 (1991); V. Bužek, P. L. Knight, and I. K. Kudryavtsev, *ibid.* **44**, 1931 (1991).
[7] L. A. Wu, M. Xiao, and H. J. Kimble, J. Opt. Soc. Am. B **4**, 1465 (1987).
[8] T. Quang, M. Kozierowski, and L. H. Lan, Phys. Rev. A **39**, 644 (1989); Z. Ficek and B. C. Sanders, Quantum Opt. **2**, 269 (1990).
[9] A. S. Shumovsky and T. Quang, J. Phys. B **22**, 131 (1989); M. R. B. Wahiddin, S. S. Hassan, J. Timonen, and R. K. Bullough, *Coherent and Quantum Optics VI,* edited by J. H. Eberly, L. Mandel, and E. Wolf (Plenum, New York, 1990), p. 1195.
[10] G. S. Agarwal and R. R. Puri, Opt. Commun. **69**, 267 (1989).
[11] M. A. Dupertuis and A. N. Kireev, Quantum Opt. **2**, 119 (1990).
[12] G. M. Palma and P. L. Knight, Phys. Rev. A **39**, 1962 (1989); A. K. Ekert, G. M. Palma, S. M. Barnett, and P. L. Knight, *ibid.* **39**, 6026 (1989); G. S. Agarwal and R. R. Puri, *ibid.* **41**, 3782 (1990); Z. Ficek, Opt. Commun. **82**, 130 (1991).
[13] S. M. Barnett and M. A. Dupertuis, J. Opt. Soc. Am. B **4**, 505 (1987).
[14] R. H. Dicke, Phys. Rev. **93**, 99 (1954).
[15] See, for example, *High-Resolution Laser Spectroscopy,* edited by K. Shimoda (Springer, Berlin, 1976).
[16] M. D. Levenson and S. S. Kano, *Introduction to Nonlinear Laser Spectroscopy* (Academic, Boston, 1988).
[17] F. DeMartini, G. Innocenti, G. R. Jacobonitz, and P. Mataloni, Phys. Rev. Lett. **59**, 2955 (1987); W. Jhe, A. Anderson, E. A. Hinds, D. Meschede, L. Moi, and S. Haroche, *ibid.* **58**, 666 (1987).
[18] B. L. Schumaker, Phys. Rep. **135**, 318 (1986); Z. Białynicka-Birula and I. Białynicki-Birula, J. Opt. Soc. Am. B **4**, 1621 (1987).
[19] M. J. Collett and C. W. Gardiner, Phys. Rev. A **31**, 3761 (1985).
[20] G. S. Agarwal, in *Quantum Optics,* edited by G. Höhler, Springer Tracts in Modern Physics Vol. 70 (Springer, Berlin, 1974), p. 25.
[21] C. Cohen-Tannoudji, in *Frontiers in Laser Spectroscopy,* edited by R. Balian, S. Haroche, and S. Liberman (North-Holland, Amsterdam, 1977), Vol. 1, p. 28.
[22] B. J. Dalton (unpublished).
[23] M. A. Dupertuis and S. Stenholm, J. Opt. Soc. Am. B **4**, 1094 (1987).
[24] J. R. Ackerhalt, P. L. Knight, and J. H. Eberly, Phys. Rev. Lett. **30**, 456 (1973); P. W. Milonni, Phys. Rep. C **25**, 1 (1976).
[25] K. Wódkiewicz and J. H. Eberly, Ann. Phys. (N.Y.) **101**, 574 (1976).
[26] L. Allen and J. H. Eberly, *Optical Resonance and Two-Level Atoms* (Wiley, New York, 1975).
[27] P. W. Milonni and P. L. Knight, Phys. Rev. A **10**, 1096 (1974).
[28] G. J. Milburn, Phys. Rev. A **34**, 4882 (1986); G. W. Ford and R. F. O'Connell, J. Opt. Soc. Am. B **4**, 1710 (1987); G. M. Palma and P. L. Knight, Opt. Commun. **73**, 131 (1989).
[29] S. Kielich, *Nonlinear Molecular Optics* (Nauka, Moscow, 1981).
[30] W. H. Louisell, *Radiation and Noise in Quantum Electronics* (McGraw-Hill, New York, 1964), p. 296.
[31] R. H. Lehmberg, Phys. Rev. A **2**, 883 (1970); M. J. Stephen, J. Chem. Phys. **40**, 669 (1964).
[32] H. Morawitz, Phys. Rev. **187**, 1792 (1969); K. H. Drexhage, Prog. Opt. **12**, 165 (1974).
[33] R. Lange, W. Grill, and W. Martienssen, Europhys. Lett.

6, 499 (1988).
[34] Z. Ficek, R. Tanás, and S. Kielich, Opt. Commun. **36**, 121 (1981); H. S. Freedhoff, Phys. Rev. A **26**, 684 (1982); Z. Ficek, *ibid.* **42**, 611 (1990).
[35] F. DeMartini, M. Marrocco, P. Mataloni, L. Crescentini, and R. Loudon, Phys. Rev. A **43**, 2480 (1991).
[36] M. Ley and R. Loudon, J. Mod. Opt. **34**, 227 (1987).
[37] M. Born and E. Wolf, *Principles of Optics* (Macmillan, New York, 1964), Chap. 7.
[38] P. W. Milonni and P. L. Knight, Opt. Commun. **9**, 119 (1973).
[39] R. G. Hulet, E. S. Hilfer, and D. Kleppner, Phys. Rev. Lett. **55**, 2137 (1985).
[40] A. Yariv, *Quantum Electronics,* 3rd ed. (Wiley, New York, 1989).